Journal of Microscopy, Vol. 198, Pt 3, June 2000, pp. 174–181.
Received 27 July 1999; accepted 31 January 2000

Direct measurement of glutathione in epidermal cells of intact *Arabidopsis* roots by two-photon laser scanning microscopy

A. J. MEYER & M. D. FRICKER
Department of Plant Sciences, University of Oxford, South Parks Road, Oxford, OX1 3RB, U.K.

Key words. *Arabidopsis* root, atrichoblast, glutathione, monochlorobimane, serial optical sections, stereology, trichoblast, two-photon laser scanning microscopy, vacuolar sequestration.

Summary

Two-photon laser scanning microscopy (TPLSM) was used to directly measure glutathione (GSH) as its fluorescent glutathione S-bimane conjugate (GSB) in developing root hair cells (trichoblasts) and non-root hair cells (atrichoblasts) of intact *Arabidopsis* roots. In comparison to confocal microscopy, TPLSM showed more detail deep within the tissue with less signal attenuation. The total level of GSB labelling reached a plateau after 60 min in both trichoblasts and atrichoblasts, reflecting depletion of GSH. GSB was formed initially in the cytoplasm and was subsequently transported into the vacuole. The volume ratio of vacuole to cytoplasm was determined using the Cavalieri estimator of volume and used to calculate the amount of GSB per volume of cytoplasm in each cell type. At the end of the time-course the cytoplasmic concentration of GSB was 2.7 ± 0.5 mM ($n = 5$) in trichoblasts and 5.5 ± 0.8 mM ($n = 5$) in atrichoblasts. In trichoblasts this value represents the initial concentration of GSH in the cytoplasm. Labelling of roots with monochlorobimane (MCB) on ice led to the formation of GSB in the cytoplasm, but prevented vacuolar sequestration. After washing prelabelled roots and transfer to room temperature, vacuolar transport resumed. Although no free MCB was present the total amount of GSB in atrichoblasts increased further, indicating that the higher values recorded in the atrichoblasts might reflect additional symplastic transport and sequestration of GSB from neighbouring cells.

Introduction

Glutathione (GSH) is the most abundant low molecular weight thiol in most organisms and plays a role in protection against environmental stresses, detoxification of xenobiotics and heavy metals, and as a reservoir of reduced sulphur that can be mobilized between different organs (for reviews see May *et al.*, 1998; Noctor *et al.*, 1998). Quantitative measurements of GSH usually involve extraction of the tissues followed by derivatization to give a chromogenic or fluorgenic compound that can be analysed by spectrophotometry or high performance liquid chromotography (HPLC). For example, reaction with monobromobimane or monochlorobimane (MCB) gives a fluorescent glutathione S-bimane conjugate (GSB) with an excitation peak at 395 nm that is suitable for HPLC analysis (Fahey & Newton, 1987). Both bimanes are membrane permeable and can also be used for fluorescent labelling of GSH *in vivo* (Coleman *et al.*, 1997a, b; Sánchez-Fernández *et al.*, 1997). In live cells or tissues, labelling with low concentrations of MCB is very slow unless it is catalysed by a glutathione S-transferase (GST), which also confers specificity for GSH above other low molecular weight or protein thiols (Shrieve *et al.*, 1988; Coleman *et al.*, 1997b). In principle, the distribution of GSB can also be visualized in tissues labelled with MCB using fluorescence microscopy (Coleman *et al.*, 1997a); however, quantitative measurements and resolution of the subcellular location require optical sectioning to remove the out-of-focus blur. We have previously shown that a distinctive labelling pattern can be observed after labelling of intact *Arabidopsis* roots with MCB and imaging using confocal laser scanning microscopy (CLSM) (Sánchez-Fernández *et al.*, 1997). One striking feature of this labelling pattern was the differential fluorescence observed in the epidermal cell layer, where cells forming root hairs (trichoblasts) were significantly brighter than the intervening non-root hair cells (atrichoblasts). In *Arabidopsis* these two different epidermal cell types are arranged in files, with the trichoblast cell files located over the anticlinal walls of the underlying cortical cells and separated from each other

Correspondence: Andreas Meyer. Tel.: + 44 1865 275060; fax: + 44 1865 275074; e-mail: Andreas.Meyer@plants.ox.ac.uk

by one or two atrichoblast cell files (Dolan *et al.*, 1993). Despite the differences in fluorescence between these two cell types it is not straightforward to correlate the difference in GSB observed with the actual cytoplasmic GSH concentration ($[GSH]_{cyt}$), as most of the GSB is transported into the vacuole as part of the normal GSH-mediated detoxification pathway. Vacuolar sequestration of GSH-conjugates is ATP-dependent and catalysed by GS-X pumps, which belong to the ATP-binding cassette super-family (Rea *et al.*, 1998). Thus, the fluorescence signal measured in the vacuole represents a combination of the original $[GSH]_{cyt}$ and dilution by the volume ratio of the vacuole to cytoplasm. In this study we examine whether the apparent difference in fluorescence between trichoblasts and atrichoblasts is related to a difference in $[GSH]_{cyt}$ which could, in turn, have functional significance in the development and physiology of these different cell types. In this study we also investigate the use of two-photon laser scanning microscopy (TPLSM) introduced by Denk *et al.* (1990) to image the GSB conjugate. Our previous imaging (Sánchez-Fernández *et al.*, 1997; Fricker *et al.*, 2000) used a modified confocal system and excitation at 442 nm with a HeCd laser (Fricker & White, 1992), which only gives about 20% excitation efficiency of the GSB (excitation $\lambda_{max} = 395$ nm). Two-photon laser scanning microscopy can be used to excite UV-fluorophors with a primary wavelength in the red or near infrared and is reported to allow deeper optical sectioning of intact tissue with less photobleaching and photodamage, greatly facilitating live-cell imaging (Xu *et al.*, 1996).

Materials and methods

Plant material

Arabidopsis thaliana var. Columbia (Col-0, Lehle Seeds, Round Rock, TX, U.S.A.) seedlings were grown vertically on root growth medium made from a basal nutrient solution pH 5.8 according to Somerville & Ogren (1982) supplemented with 1% sucrose and with 1% Phytagel (Sigma, Poole, U.K.) as a gelling agent. Seeds were surface sterilized in 70% ethanol, washed twice in sterile water and plated on Phytagel plates. Plates were stored at 5 °C for 2 days and then transferred to a growth cabinet at 21 °C with a 16 h light/8 h dark regime. All experiments were carried out with 5-day-old seedlings.

Fluorescent dyes

Stock solutions of 100 mM MCB were prepared in dimethyl sulphoxide and stored at −20 °C. Aliquots were thawed immediately prior to use and diluted to a final concentration of 20–300 μM in basal nutrient solution. Propidium iodide (PI) was prepared as 5 mM aqueous stock solution and used at a final concentration of 20–50 μM. All dyes were obtained from Molecular Probes (Eugene, OR, U.S.A.).

Laser scanning microscopy

Intact seedlings were transferred to a drop of MCB solution on a microscope slide and covered with a coverslip using 150 μm thick spacers to avoid squashing the roots. Roots were imaged using a MRC-1024MP (Bio-Rad Microscience Ltd, Hemel Hempstead, U.K.) attached to an upright microscope (BX50WI, Olympus, Southall, U.K.) using an Olympus 60× UPlanApo 1.2 NA water immersion lens. Single photon excitation was achieved with a 442-nm HeCd laser (Liconix, Santa Clara, CA, U.S.A.) coupled into the MRC-1024MP scan head by a fibre-optic. Fluorescence of GSB and PI was recorded on internal detectors at 522 ± 17.5 nm (GSB) and with a 585 nm long pass filter (PI). The confocal aperture was set to 1.5–2.0 mm. Two-photon excitation was achieved using a tuneable femtosecond pulsed mode-locked Ti : Sapphire laser (Mira 900, Coherent, Cambridge, U.K.) equipped with a 5 W solid state pump laser (Verdi, Coherent). The laser was operated at 770 nm with ~100 fs pulse width and a pulse repetition rate in the range 50–100 MHz. Fluorescence was collected simultaneously using two non-descanned (external) detectors separated by a 550 nm dichroic and a 480 ± 30 nm interference filter for GSB and a 605 ± 45 nm interference filter for PI. Additionally, the PI channel was equipped with a 575 ± 75 nm blocking filter to remove any reflected infrared light. Images were collected in Lasersharp (Bio-Rad Microsciences) with a pixel spacing of 0.192–0.386 μm and Kalman averaged over four frames. Changes in fluorescence intensity over time were measured for regions of interest in the cytoplasm and vacuole after alignment of the (x, y, t)-stacks in Scion Image™ (Scion, Frederick, MD, U.S.A.). Image montages were assembled using Photoshop™ (Adobe Systems, San Jose, CA, U.S.A.).

Calibration of the GSB fluorescence

A 10-mM stock solution of GSB was made from 10 mM MCB and 100 mM GSH in the presence of a glutathione S-transferase (Rabbit Liver GST, Sigma, Poole, U.K.). Excess GSH and GST were used to ensure that all MCB was conjugated. A dilution series was made from this stock and four or five different concentrations of GSB were routinely used for calibration.

Measurement of the volume of subcellular compartments

The volume of the cytoplasm and vacuole were measured using the Cavalieri estimator of volume (Digital Stereology™, Kinetic Imaging, Liverpool, U.K.) from uniform random sections extracted from stacks of serial optical

sections collected at 1 μm focus increments through the epidermal cells. Roots were labelled with 100 μM MCB and imaged either early in the time-course or in the presence of 1 mM sodium azide, when the fluorescence was mainly restricted to the cytoplasm, or after 120 min when the GSB was predominantly in the vacuole. Propidium iodide (20–50 μM) was used to label cell walls immediately prior to the imaging.

Results

Fluorescence from GSB was readily imaged in optical sections of intact *Arabidopsis* roots using either single photon excitation at 442 nm (Fig. 1a, c, e) or two-photon excitation at 770 nm (Fig. 1b, d, f). Propidium iodide fluorescence was collected simultaneously with the GSB signal and, although neither excitation wavelength was optimal to excite PI, the labelling was sufficiently strong to allow clear visualization of the cell walls and tissue architecture (PI signal not shown in Fig. 1; see Figs 2a and 3). No labelling of nuclei was observed with PI, indicating that plasma membrane integrity was not compromised during the labelling and imaging procedures, even in extended time-courses or during collection of 3-D images (Fig. 2a).

The fluorescence signal was attenuated to a similar extent for both CLSM with excitation at 442 nm and TPLSM with excitation at 770 nm (Fig. 1e, f). However, the amount of blurring with increasing depth into the root was lower using TPLSM and 770 nm excitation (Fig. 1b, f) compared to CLSM and 442 nm excitation (Fig. 1a, e). Within the dense, meristematic tissue at the root apex, mid-plane optical (x, y) sections taken by TPLSM (Fig. 1b) showed higher contrast than the equivalent sections taken by CLSM (Fig. 1a). In a similar manner bright, well-defined features were observed within the vascular tissue in optical (x, z) cross-sections through the elongation zone (Fig. 1f), which could not be resolved by CLSM (Fig. 1e). With either CLSM or TPLSM, trichoblast and atrichoblast cell files were labelled differentially, with atrichoblasts being significantly brighter after labelling with MCB (Fig. 1c–f). Owing to the significantly enhanced contrast, TPLSM revealed many more subcellular details than CLSM. This enabled clear separation of vacuole and cytoplasm, including cytoplasmic strands through the vacuole (Figs 2a and 3). This allowed more accurate measurement of subcellular compartment volumes in comparison to images collected by CLSM.

Fluorescence from GSB was observed to increase initially in the cytoplasm and then transferred into the vacuole over time in both trichoblasts and atrichoblasts (Fig. 2a). The fluorescence level was measured from both compartments and this confirmed that there was a transient increase in fluorescence in the cytoplasm coupled to a steady rise in vacuolar fluorescence to a plateau after about 60 min

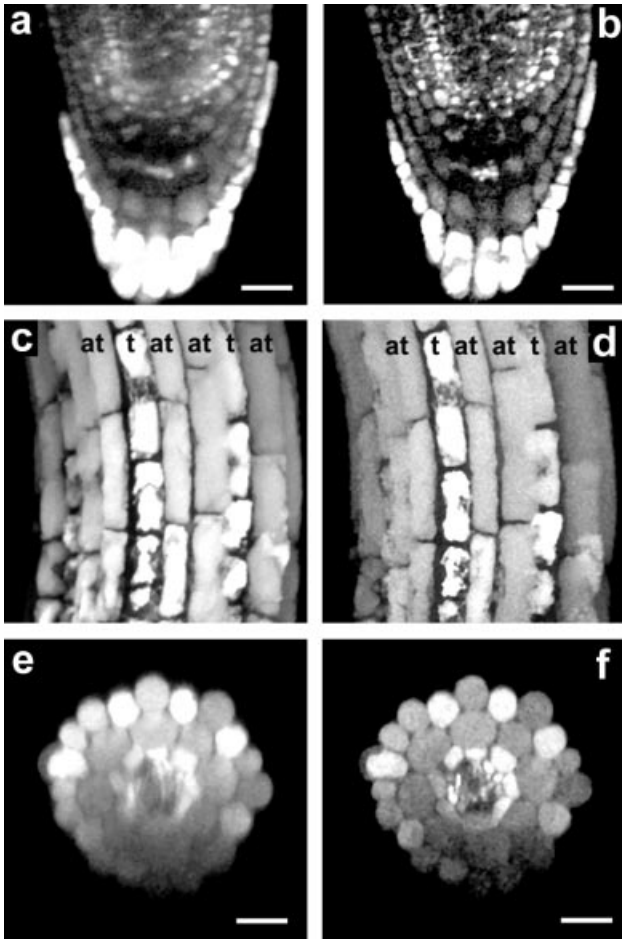

Fig. 1. Comparison between confocal and two-photon imaging of intact *Arabidopsis* roots labelled with monochlorobimane. 3-D images were collected using confocal laser scanning microscopy with excitation at 442 nm (a, c, e) or two-photon laser scanning microscopy with excitation at 770 nm (b, d, f) of an intact root labelled with 100 μM MCB. (a) and (b) show single optical (x, y) sections through the mid-plane of the root tip taken from a stack of 120 images collected at 1 μm intervals. (c) and (d) show the differential labelling of the trichoblasts (t) and atrichoblasts (at) cell files in maximum projections of the elongation zone from the same root as in (a) and (b). (e) and (f) show vertical (x, z) sections in a comparable region in the elongation zone of a different root. All scale bars = 20 μm.

(Fig. 2b). The fluorescence intensities were calibrated against GSB standards imaged under the same conditions (Fig. 2b, inset) and indicated that the average vacuolar concentration of GSB in the trichoblasts was 1.6 ± 0.3 mM (n = 5) and in the atrichoblasts 2.4 ± 0.4 mM (n = 5) (Fig. 2b). To test whether the calibration for GSB might differ between the cytoplasm and the vacuole, the sensitivity of the fluorophore to varying pH, ionic strength and hydrophobicity was measured. The fluorescence emission of GSB was not markedly affected by pH between pH 5 and

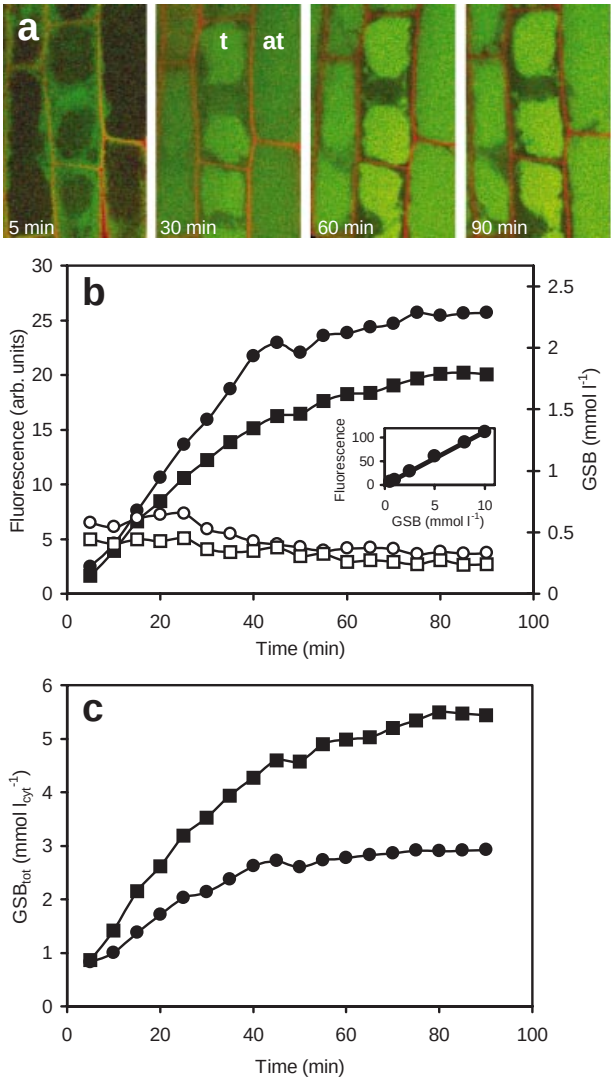

Fig. 2. Time course of labelling and sequestration of GSB in trichoblast and atrichoblast cells of an *Arabidopsis* root. (a) Representative optical sections showing the increase in GSB fluorescence (green) initially in the cytoplasm and subsequently in the vacuole of trichoblast (t) and atrichoblast (at) cells in the elongation zone. Cell walls were simultaneously visualized with 50 μM propidium iodide (red). Four images are shown from a series of 18 images collected at 5 min intervals after the start of the labelling with 100 μM MCB using TPLSM with excitation at 770 nm. (b) Traces showing the change in average GSB fluorescence intensity in the cytoplasm (open symbols) and vacuole (closed symbols) of trichoblast (○, ●) and atrichoblast (□, ■) cells in time. Calibrated values on the right-hand axis were derived from the linear calibration (inset). (c) Traces showing the integrated amount of GSB formed in the cytoplasm. Calibrated values from the cytoplasm and vacuole were summed taking into account the volume ratio between cytoplasm and vacuole for trichoblast (●) and atrichoblast (■) cells. Traces shown in (b) and (c) show data from one cell in a single root. Plotted data are representative of five separate experiments on five roots.

pH 9, or changes in the ionic strength from 0 to 1 M (Table 1); however, increasing the hydrophobicity of the solution by adding ethanol led to a slight increase in fluorescence (Table 1). Thus, addition of 10% ethanol caused an increase in fluorescence of about 20%, but the effect appeared to saturate, as further increasing the ethanol concentration to 25% caused only an additional 6% increase in fluorescence. Levels of autofluorescence in the absence of MCB were negligible in the cytoplasm and vacuole with excitation at either 770 nm or 442 nm (data not shown).

To calculate the total amount of GSB formed in the cytoplasm during the labelling period, the relative volumes of the cytoplasm and vacuole for both cell types were measured using the Cavalieri estimator from 3-D (x, y, z) images of cells from the same region of the root. In two out of five time-course experiments volume measurements were taken from the same cells that were used for the analysis of GSB concentration. Stacks of serial optical sections were collected at a z-step of 1 μm (Fig. 3a). Every fifth section was extracted from a randomised start position (Fig. 3b), overlaid with a randomly positioned grid (Fig. 3c), and the pixel at the apex of each grid marker was manually assigned to cytoplasm, vacuole or cell wall. Using this approach, the relative volume of cytoplasm in trichoblasts and atrichoblasts in the elongation zone was estimated to be 47% and the vacuole 53%. In atrichoblasts the cytoplasm was 26% and the vacuole 74% of the total cell volume. These estimates of volumes were used to calculate the apparent amount of GSB formed in the cytoplasm and gave values of 5.5 ± 0.8 mM ($n = 5$) for atrichoblasts and 2.7 ± 0.5 mM ($n = 5$) for trichoblasts (Fig. 2c). When buthionine sulfoximine, a known inhibitor of GSH synthesis, was added to the dye solution, plateau values reached 5.2 ± 0.6 mM ($n = 4$) for atrichoblasts and 2.9 ± 0.9 mM ($n = 4$) for trichoblasts.

The higher value of $[GSB]_{cyt}$ calculated for the atrichoblasts might reflect a genuinely higher level of cytoplasmic GSH in this cell type or might arise from import and sequestration of GSB from neighbouring, symplastically connected cells. To test the latter possibility, roots were incubated with 100–300 μM MCB on ice for 30 min and washed twice with ice-cold medium to remove residual free dye. In preliminary experiments it was shown that no free MCB was detectable in the wash solution after this procedure. Under these conditions, GSH was labelled up in the cytoplasm but vacuolar transport was significantly reduced compared to roots labelled at room temperature. Vacuolar transport activity resumed immediately after transferring roots to room temperature, and after 25 min most of the fluorescence was sequestered into the vacuole in both cell types (Fig. 4a, c). In trichoblasts, the total amount of GSB per volume of cytoplasm remained constant over 60 min after transfer to room temperature and was calculated as 2.3 ± 0.4 mM ($n = 5$) (Fig. 4b). By contrast,

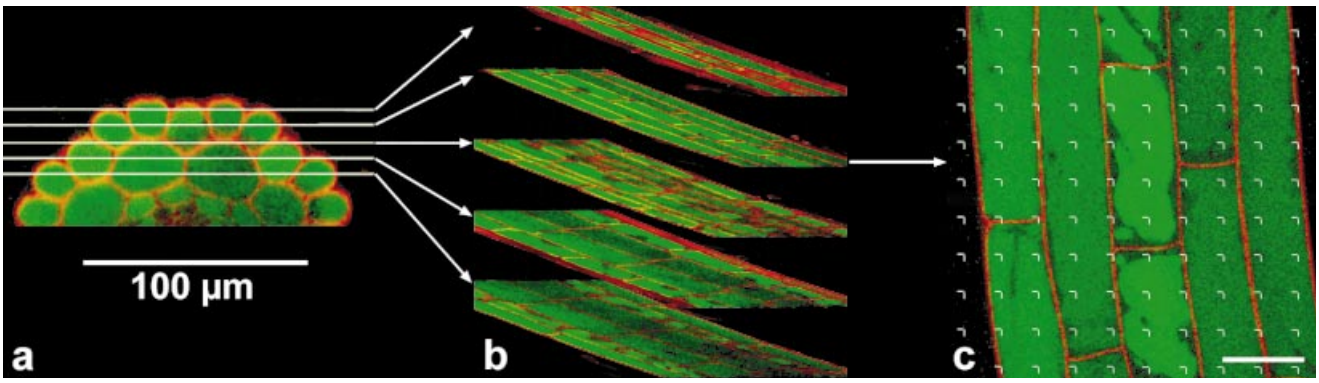

Fig. 3. Stereological approach to estimate the volume of subcellular compartments in epidermal cells of an *Arabidopsis* root from serial optical sections captured by TPLSM. (a) Optical (x, z) cross-section through an intact root labelled with 20 µM MCB for 1 h and 50 µM PI immediately prior to the imaging showing GSB fluorescence (green) and cell wall labelling with PI (red). The white lines give the planes of the horizontal optical (x, y) sections displayed in (b). (b) A series of horizontal optical (x, y) sections were selected with a random start position and uniform sample increment of 5 µm from a 3-D (x, y, z) stack of 40 optical sections collected at 1 µm intervals. Five representative images are shown after 40° rotation and at a tilt angle of 75°. The distance between the displayed sections is 8 µm. (c) Single optical section (x, y) with an overlaid point grid used for estimation of cytoplasmic and vacuolar volume fractions in different cell types. Scale bar = 20 µm.

atrichoblasts showed an increase in total GSB per volume of cytoplasm during the first 25 min, from 3.5 ± 0.7 mM to 5.2 ± 1.0 mM (n = 5) (Fig. 4d). This increase was not due to continued conjugation as MCB was no longer present after the wash stages. After 25 min the total amount of GSB in the atrichoblasts did not change significantly.

Discussion

Several features of TPLSM combine to allow imaging deeper into highly scattering biological tissues and generate images with enhanced contrast in comparison with CLSM. Near-infrared light typically penetrates biological material significantly better than blue or UV light with less scattering and refraction (Duck, 1990). In addition, as the optical sectioning is defined by the monochromatic illumination the constraints on the emission light path are relaxed and it is possible to use wide-field collection with external detectors (Denk *et al.*, 1990). In this study, improved contrast was noted when images were collected from deep within the root using TPLSM at 770 nm in comparison to CLSM at 442 nm. Equally, however, significant attenuation was still observed even through a relatively thin plant specimen (≈100 µm) with TPLSM. We have not quantified the relative extent of this attenuation but estimate that TPLSM is approximately 10–20% better at 50 µm than CLSM. In absolute terms, the estimated signal attenuation through the epidermal cell layer would be around 8%. The enhanced contrast achieved by TPLSM allowed clear separation of cytoplasm and vacuole in epidermal cells under investigation and enabled determination of the volume ratio of these two compartments.

The ability to measure a metabolite such as GSH at the cellular level by TPLSM overcomes some of the limitations inherent with conventional biochemical techniques, which require extraction of the tissue and therefore give average levels in whole tissues. Using MCB to label *Arabidopsis* roots, Sánchez-Fernández *et al.* (1997) showed a marked cellular heterogeneity in the labelling pattern that would be lost in a biochemical assay for GSB levels. This study confirms the difference in fluorescence intensity observed between trichoblasts and atrichoblasts in the root epidermis.

The fluorescence of GSB increased to a plateau value, which reflects complete depletion of the cytoplasmic GSH pool. The fluorescence at this point therefore contains information about the concentration of GSH initially present

Table 1 Effect of pH, ionic strength and hydrophobicity on the fluorescence intensity of 10 µM GSB (λ_{ex} = 442 nm, λ_{em} = 477 nm; n = 5). Intensity values are given as percentage of the values measured at pH 7.0, ionic strength = 0 mol L^{-1} or 0% EtOH, respectively.

	pH					Ionic strength (mol L^{-1})					EtOH (%)		
	5.0	6.0	7.0	8.0	9.0	0	0.1	0.25	0.5	1.0	0	10	25
Intensity (%)	104.3 ± 5.0	105.3 ± 6.0	100	100.1 ± 3.5	102.6 ± 3.6	100	100.2 ± 7.1	99.1 ± 2.8	100.5 ± 3.2	101.8 ± 4.8	100	120.5 ± 6.3	126.4 ± 5.9

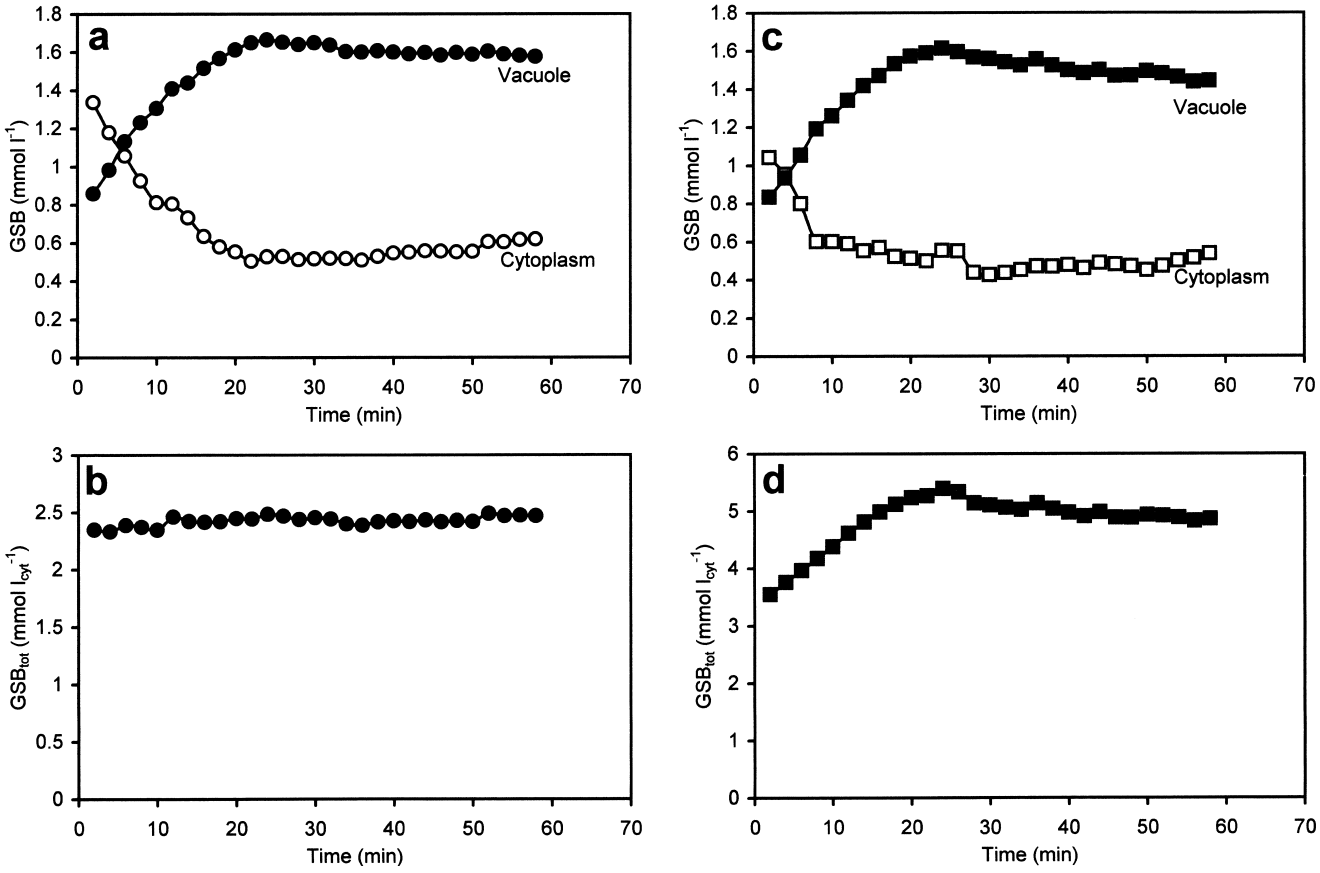

Fig. 4. Typical time courses for the transport of GSB into the vacuole of epidermal cells after prelabelling *Arabidopsis* roots with 300 μM MCB on ice for 30 min. (a) and (c) Changes in cytoplasmic (open symbols) and vacuolar (closed symbols) GSB concentrations in a trichoblast (a) and an atrichoblast (c) cell. (b) and (d) Total GSB concentration expressed per volume of cytoplasm in a trichoblast (b) and an atrichoblast (d) cell. Values were calculated from (a) and (c) using the volume ratio of vacuole to cytoplasm determined using the Cavalieri estimator of volume. All graphs are representative of five separate experiments on different roots.

in the cytoplasm; however, the GSB fluorescence was diluted by sequestration into the vacuole. As the fluorescence of GSB was not markedly affected by its environment, the calibrated fluorescence only had to be corrected for dilution due to the larger volume of the vacuole compared with the cytoplasm. To convert calibrated GSB fluorescence in the vacuole and cytoplasm to $[GSH]_{cyt}$ involved measurement of the volume ratio between both compartments. Application of stereological techniques to stacks of serial optical sections provides a rapid and reliable route to measure the volume of subcellular compartments (Howard & Reed, 1998; Kubínová *et al.*, 1999). Here we used the Cavalieri estimator of volume to measure the volume ratio of vacuole to cytoplasm. The data provided quantitative confirmation of the delay in vacuolation in trichoblasts compared with atrichoblasts at the same distance from the root tip (Dolan *et al.*, 1994; Galway *et al.*, 1994).

Taking into account the volume ratio of vacuole to cytoplasm, around 3 mM GSB was formed in the cytoplasm of the trichoblast cells. Inclusion of buthionine sulfoximine, an inhibitor for GSH synthesis, did not alter the endpoint of the labelling kinetics, indicating that no *de novo* GSH synthesis took place during the assay period. Therefore the integrated amount of GSB formed in the cytoplasm reflects the $[GSH]_{cyt}$ at the beginning of the experiment. There are to date virtually no comparable estimates of cytoplasmic concentrations of GSH in plants, as most measurements have been done after extraction of GSH from whole tissues. Expressed on a fresh weight basis these values range from 200 to about 2500 nmol $(g\ FW)^{-1}$ (Smith *et al.*, 1989; Rauser *et al.*, 1991; Noctor *et al.*, 1996; Xiang & Oliver, 1998). Estimates of $[GSH]_{cyt}$ calculated from these measurements based on the water content of the tissue and percentage cytoplasm range from 100 μM to more than 10 mM, depending on the tissue, the physiological condition and seasonal influences. Our own measurements of $[GSH]_{cyt}$ in groups of cells in *Arabidopsis* roots gave values between 2 and 3 mM for most cell types (Fricker *et al.*, 2000).

In atrichoblasts the amount of GSB per volume of cytoplasm appeared to be twice as high as in the

trichoblasts. This would suggest that neighbouring cells could maintain substantially different $[GSH]_{cyt}$. In the meristem, most cells are interconnected by plasmodesmata, which allow rapid movement of low molecular weight molecules from one cell into another (Robards & Lucas, 1990; Kragler *et al.*, 1998). Increasing symplastic isolation of epidermal cells during their differentiation process by shutting down plasmodesmata would allow us to establish different concentration of low molecular weight metabolites such as GSH between the two cell types. Alternatively, the differences in total GSB observed may reflect a combination of labelling the initial $[GSH]_{cyt}$ in atrichoblasts and import and sequestration of GSB from symplastically connected cells. Dye-coupling experiments showed that cells in the root epidermis of *Arabidopsis* become progressively isolated during development (Duckett *et al.*, 1994). The fact that trichoblasts and atrichoblasts show different amounts of GSB might suggest that trichoblasts become symplastically isolated from underlying cortex cells earlier in development than atrichoblasts. Support for this interpretation comes from the low temperature pulse-chase experiments where all the GSH pool was labelled under conditions that prevented vacuolar sequestration. Plants grown under low temperature conditions are known to contain increased levels of GSH (Anderson *et al.*, 1992). However, transfer of maize plants from 25 °C to 5 °C does not change the total pool of GSH and its redox state significantly within the first 4 h (Leipner *et al.*, 1997). Furthermore, the activity of glutathione reductase in maize was shown to be insensitive to suboptimal temperature (Kocsy *et al.*, 1996). In this study the total level of GSB after the cold treatment was similar to the control. During the recovery period no further GSB labelling could occur in the absence of MCB; however, redistribution of preformed GSB was observed. Under these conditions the increase in GSB in the atrichoblasts might reflect import from the underlying cortex cells if the efficiency of the vacuolar GS-X pumps in epidermal cells was greater than in the cortical cells. These results emphasize the advantages of techniques capable of investigating cells in their correct tissue context and may enable mapping of xenobiotic detoxification at the cellular level using MCB as a model xenobiotic.

Acknowledgements

We would like to thank Mark Browne and Kinetic Imaging Ltd for providing a beta-version of their Stereology software package. We are grateful to Nick White and the Plant Sciences/Bio-Rad Biological Microscopy Unit (BMU) for technical support in using two-photon laser scanning microscopy. This work was funded by Rhône-Poulenc Agriculture Ltd.

References

Anderson, J.V., Chevone, B.I. & Hess, J.L. (1992) Seasonal variation in the antioxidant system of eastern white pine needles. Evidence for thermal dependence. *Plant Physiol.* **98**, 501–508.

Coleman, J.O.D., Blake-Kalff, M.M.A. & Davies, T.G.E. (1997a) Detoxification of xenobiotics by plants: chemical modification and vacuolar compartmentation. *Trends Plant Sci.* **2**, 144–151.

Coleman, J.O.D., Randall, R. & Blake-Kalff, M.M.A. (1997b) Detoxification of xenobiotics in plant cells by glutathione conjugation and vacuolar compartmentalization: a fluorescent assay using monochlorobimane. *Plant Cell Environ.* **20**, 449–460.

Denk, W., Strickler, J. & Webb, W.W. (1990) Two-photon laser scanning microscopy. *Science*, **248**, 73–76.

Dolan, L., Janmaat, K., Willemsen, V., Listead, P., Poethig, S. & Roberts. & Scheres, B. (1993) Cellular organisation of the *Arabidopsis thaliana* root. *Development*, **119**, 71–84.

Dolan, L., Duckett, C.M., Grierson, C., Linstead, P., Schneider, K., Lawson, E., Dean, C. & Roberts, K. (1994) Clonal relationships and cell patterning in the root epidermis of *Arabidopsis*. *Development*, **120**, 2465–2474.

Duck, F.A. (1990) *Physical Properties of Tissue.* Academic Press, London.

Duckett, C.M., Oparka, K.J., Prior, D.A.M., Dolan, L. & Roberts, K. (1994) Dye-coupling in the root epidermis of *Arabidopsis* is progressively reduced during development. *Development*, **120**, 3247–3255.

Fahey, R.C. & Newton, G.L. (1987) Determination of low-molecular-weight thiols using monobromobimane fluorescent labeling and high-performance liquid chromatography. *Meth. Enzymol.* **143**, 85–96.

Fricker, M.D. & White, N.S. (1992) Wavelength considerations in confocal microscopy of botanical specimens. *J. Microsc.* **166**, 29–42.

Fricker, M.D., May, M., Meyer, A.J., Sheard, N. & White, N.S. (2000) Measurement of glutathione levels in intact roots of *Arabidopsis*. *J. Microsc.* **198**, 162–173.

Galway, M.E., Masucci, J.D., Lloyd, A.M., Walbot, V., Davis, R.W. & Schiefelbein, J.W. (1994) The *TTG* gene is required to specify epidermal cell fate and cell patterning in the *Arabidopsis* root. *Dev. Biol.* **166**, 740–754.

Howard, C.V. & Reed, M.G. (1998) *Unbiased Stereology.* BIOS Scientific Publishers. Oxford.

Kocsy, G., Brunner, M., Rüegsegger, A., Stamp, P. & Brunold, C. (1996) Glutathione synthesis in maize genotypes with different sensitivities to chilling. *Planta*, **198**, 365–370.

Kragler, F., Lucas, W.J. & Monzer, J. (1998) Plasmodesmata: dynamics, domains and patterning. *Ann. Bot.* **81**, 1–10.

Kubínová, L., Janácek, J., Guilak, F. & Opatrný, Z. (1999) Comparison of several digital and stereological methods for estimating surface area and volume of cells studied by confocal microscopy. *Cytometry*, **36**, 85–95.

Leipner, J., Fracheboud, Y. & Stamp, P. (1997) Acclimation by suboptimal growth temperature diminishes photooxidative damage in maize leaves. *Plant Cell Enivron.* **20**, 366–372.

May, M.J., Vernoux, T., Leaver, C., Van Montagu, M. & Inzé, D. (1998) Glutathione homeostasis in plants: implications for

environmental sensing and plant development. *J. Exp. Bot*. **49**, 649–667.

Noctor, G., Strohm, M., Jouanin, L., Kunert, K.-J., Foyer, C.H. & Rennenberg, H. (1996) Synthesis of glutathione in leaves of transgenic poplar overexpressing γ-glutamylcysteine synthetase. *Plant Physiol*. **112**, 1071–1078.

Noctor, G., Arisi, A.-C.M., Jouanin, L., Kunert, K.-J., Rennenberg, H. & Foyer, C.H. (1998) Glutathione: biosynthesis, metabolism and relationship to stress tolerance explored in transformed plants. *J. Exp. Bot*. **49**, 623–647.

Rauser, W., Schupp, R. & Rennenberg, H. (1991) Cysteine, γ-glutamylcysteine, and glutathione levels in maize seedlings. Distribution and translocation in normal and cadmium exposed plants. *Plant Physiol*. **97**, 128–138.

Rea, P.A., Li, Z.-S., Lu, Y.P., Drozdowicz, Y.M. & Martinoia, E. (1998) From vacuolar GS-X pumps to multispecific ABC transporters. *Annu. Rev. Plant Physiol. Plant. Mol. Biol*. **49**, 727–760.

Robards, A.W. & Lucas, W.J. (1990) Plasmodesmata. *Annu. Rev. Plant Physiol. Plant Mol. Biol*. **41**, 369–420.

Sánchez-Fernández, R., Fricker, M.D., Corben, L.B., White, N.S., Sheard, N., Leaver, C.J., Van Montagu, M., Inzé, D. & May, M.J. (1997) Cell proliferation and hair tip growth in the *Arabidopsis* root are under mechanistically different forms of redox control. *Proc. Natl. Acad. Sci. USA*, **94**, 2745–2750.

Shrieve, D.C., Bump, E.A. & Rice, G.C. (1988) Heterogeneity of cellular glutathione among cells derived from a murine fibrosarcoma or a human renal cell carcinoma detected by flow cytometry analysis. *J. Biol. Chem*. **263**, 14107–14114.

Smith, I.K., Vierheller, T.L. & Thorne, C.A. (1989) Properties and functions of glutathione reductase in plants. *Physiol. Plant*. **77**, 449–456.

Somerville, C.R. & Ogren, W.L. (1982) Isolation of photorespiration mutants in *Arabidopsis*. *Methods in Chloroplast Molecular Biology* (ed. by M. Edelman, R. B. Hallick and N. H. Chua), pp. 129–138. Elsevier Biomedical Press, Amsterdam.

Xiang, C. & Oliver, D.J. (1998) Glutathione metabolic genes coordinately respond to heavy metals and jasmonic acid in *Arabidopsis*. *Plant Cell*, **10**, 1539–1550.

Xu, C., Zipfel, W., Shear, J.B., Williams, R.M. & Webb, W.W. (1996) Multiphoton fluorescence excitation: new spectral windows for biological nonlinear spectroscopy. *Proc. Natl. Acad. Sci. USA*, **93**, 10763–10768.